Article

Not peer-reviewed version

Physicochemical and Mineralogical Characterizations of Two Natural Laterites from Burkina Faso: Assessing Their Potential Usage as Adsorbent Materials

Corneille Bakouan , Louise Chenoy , Boubié Guel * , Anne-LIse Hantson

Posted Date: 27 February 2025

doi: 10.20944/preprints202502.2150.v1

Keywords: Natural laterites; sorption properties; mineralogy; anionic exchange capacity

 doi:10.20944/preprints202502.2150.v1

Article

Physicochemical and Mineralogical Characterizations of Two Natural Laterites from Burkina Faso: Assessing Their Potential Usage as Adsorbent Materials

Corneille Bakouan [1,2,3], Louise Chenoy [3], Boubié Guel [2,*] and Anne-Lise Hantson [3]

[1] Université de Lédéa Bernard OUEDRAOGO, Laboratoire de Recherche et de Développement (LRD), Ouahigouya 01 BP 346, Burkina Faso

[2] Université Joseph KI-ZERBO, Laboratoire de Chimie Moléculaire et des Matériaux (LCMM), U.F.R –SEA/, 03 BP 7021 Ouaga 03, Burkina Faso

[3] Université de Mons, Faculté Polytechnique, Service de Génie des Procédés Chimiques et Biochimiques, Place du Parc 20, 7000 Mons, Belgique

* Correspondence: boubieguel@yahoo.fr and boubie.guel@ujkz.bf; Tel: +00226-76645044

Abstract: In the framework of lateritic material valorization, we demonstrated how the geological environment determines the mineralogical characterizations of two laterite samples, KN and LA. KN and LA originate from the Birimian and Precambrian environments, respectively. We showed that the geological criterion alone does not determine the applicability of these laterites as potential adsorbents but must be associated with their physicochemical properties. The characterizations were carried out using Fourier Transform Infrared Spectroscopy (FTIR), X-ray Diffraction (XRD), Thermal analysis, and Atomic Emission Spectrometry Coupled with an Inductive Plasma Source. ICP analyses indicated that the chemical composition of the laterite samples comprised major oxides (SiO_2, Al_2O_3, and Fe_2O_3) as well as minor oxides (Na_2O, K_2O TiO_2) in KN and LA samples. The major mineral phases obtained by X-ray diffraction analysis coupled with infrared analysis showed that KN and LA laterite samples were composed of hematite (13.36% to 11.43%), goethite (7.44% to 6.31%), kaolinite (35.64% to 17.05%) and quartz (33.58% to 45.77%). The anionic exchange capacity of the KN and LA laterites ranged from 86.50 ± 3.40 to 73.91 ± 9.94 cmol(-).kg^{-1} and 73.59 ± 3.02 to 64.56 ± 4.08 cmol(-).kg^{-1}, respectively. The specific surface values determined by the BET method were 58.65 m^2/g and 41.15 m^2/g for KN and LA samples, respectively. Based on their physicochemical and mineralogical characteristics, KN and LA laterite samples were shown to possess a high potential as adsorbent material candidates for removing heavy metals and/or anionic species from groundwater.

Keywords: natural laterites; sorption properties; mineralogy; anionic exchange capacity

1. Introduction

Laterites constitute a large family of soils typical of humid tropical regions. They originate from the alteration process of a bedrock, which is depleted in silica and enriched in iron oxide and alumina. They are products of intense meteoric weathering and consist of a mineral assemblage of goethite, hematite, aluminum hydroxide, kaolinite, and quartz [1–3]. Chemically, the structure of lateritic materials contains a high percentage of iron oxide (Fe_2O_3), alumina (Al_2O_3), and silica (SiO_2) mineral phases, which are present as a combination consisting of Fe_2O_3 – Al_2O_3 – SiO_2 – H_2O matrices [3]. The $SiO_2/(Al_2O_3 + Fe_2O_3)$ ratio compared to that of the parent rock must be in such a way that the laterite formation does not contain more silica than the one which is retained in the remaining quartz and which is only necessary for the formation of kaolinite [4]. Moreover, laterites occur in nature with various yellow, brown, and red residual solids of nodular gravels and fine-grained and/or cemented

 doi:10.20944/preprints202502.2150.v1

solids. Laterites can vary from loose red sand to massive hard rock; sometimes, both forms coexist. The characteristic red color appears due to the presence of iron compounds in laterite. The composition of laterite varies significantly depending on the extent of laterization, the source rock, and the geographic location [5,6].

Laterites have been the subject of diverse applications reported in the literature [7–12]. They have been widely used in road construction in tropical and equatorial African countries, as well as in South America, whether they are lateritic gravels, lateritic clays, lateritic shells, or crusts [1,13,14]. They were also shown to be efficient adsorbents in treating water contaminated by inorganic pollutants. In several countries such as India, Vietnam, and Bangladesh, they have been used with great satisfaction in the adsorption of arsenic [8,9,15–17]. We recently reported their application for arsenic removal in Burkina Faso [2]. According to the literature, the efficiency of these materials as best adsorbent candidates for the removal of inorganic and organic pollutants is only highlighted by their physicochemical and structural characteristics: the specific surface area, the anion exchange capacity, the cation exchange capacity, and the composition, which is made up mostly of iron and aluminum oxides. These characteristics appeared to be the most critical and were highlighted in several studies on clay and/or lateritic minerals used to remove inorganic or organic pollutants [11,12,18–20]. Using laterites and/or clays as adsorbents has several advantages over many other adsorbents available in nature in terms of low-cost process, abundant availability, high specific surface area, excellent adsorption properties, non-toxic nature, and great ion exchange potential. Their applications depend closely on their structure, composition, and physicochemical characteristics. Being aware of these characteristics is decisive for better exploitation and probably opens up new application areas [21].

In the literature, various techniques, such as X-ray powder diffraction (XRPD), Fourier transform infrared (FT-IR) spectroscopy, scanning electron microscopy (SEM), chemical analysis, cation exchange capacity (CEC), and specific surface area (BET) have been carried out to investigate the laterite characterization processes because of the removal of inorganic pollutants [7,9–11,22–24]. Although numerous studies have been conducted on the characterization of natural laterites for the sorption of heavy metals and/or metalloids [8,9,24–26], few of them have explored the relationship between their physicochemical and mineralogical properties and their adsorptive properties. Therefore, in-depth studies are required in terms of characterization techniques such as anion exchange capacity (AEC), cation exchange capacity (CEC), X-ray powder diffraction (XRPD), Fourier transform infrared spectroscopy (FT-IR), and scanning electron microscopy (SEM) to analyze the parameters, which are responsible for the sorption of inorganic pollutants. It should be emphasized that XRPD analysis, infrared spectroscopy (IR), SEM analysis, CEC, and AEC are among the most informative techniques to characterize laterites and to collect information on their potential usage as adsorbents for the removal of inorganic pollutants from aqueous matrices.

XRPD analysis has been used to determine the presence of mineral phases such as goethite, hematite, and kaolinite in laterites used in the adsorption of inorganic pollutants [9–11,16]. Nayanthika et al. reported that iron and aluminum oxide-rich laterites are effective in aqueous solution [27]. Other authors have made similar observations using laterites for adsorption of inorganic pollutants [7,9,10,16].

FT-IR spectroscopy was used to prove the presence of specific functional groups on the surface of laterites used in the adsorption of inorganic pollutants [28–30]. It was reported that the FT-IR peaks of laterites, which are related to the characteristic vibrations of the goethite and hematite bonds, appeared around 798 cm^{-1}, 1004 cm^{-1}, 681 cm^{-1} and 460 cm^{-1}, 535 cm^{-1}, 472 cm^{-1} for goethite and hematite, respectively [6,9,28,30,31].

SEM analysis was used to observe the morphology of natural laterites that remove inorganic pollutants. Ghani et al. showed the presence of pores and cavities on the surface of adsorbents through SEM images of laterites, which are key factors for removing inorganic pollutants from water by adsorption [23]. Nguyen et al. and Thanakunpaisit et al. confirmed the presence of mineral phases present in laterites detected by XRPD, such as goethite, hematite, and kaolinite in laterites [8,9,16].

 doi:10.20944/preprints202502.2150.v1

Differential scanning calorimetry (DSC) is a complementary technique to observe thermal phenomena. These phenomena are characteristic of a mineral phase, corresponding to a transformation of goethite into hematite. Several authors have observed these phenomena in clay materials [13,32]. However, few studies combine the DSC characterizations of laterites with their physicochemical and structural characteristics.

The cation exchange capacity (CEC) is one of the fundamental properties of clay minerals. This parameter is important in several studies of clay minerals that remove cationic pollutants [18–20,33] and can be determined routinely. Laterites or clays, having a high cation exchange capacity, can effectively retain unwanted ions and thus prevent them from contaminating the environment or drinking water sources. Many mechanisms have been postulated for metal ion adsorption onto clay minerals. Among them, it is generally admitted that the adsorption of metal ions appeared to involve an ion exchange reaction at permanent charge sites due to the high value of cation exchange capacity [18]. However, CEC values for natural laterites have not been primarily reported in the literature.

The anionic exchange capacity (AEC) is generally omitted in most studies reporting the use of natural laterites for pollutant removal. Several researchers have reported the physicochemical and mineralogical properties of natural materials (laterites) in removing inorganic pollutants without paying close attention to their anion exchange capacity [6,8,12,15,34–41]. It is known that the AEC is an important property that could explain the adsorption of anionic pollutants. Lawrinenko et al. determined the anion exchange capacity of biochars produced from three raw materials at 500 and 700 °C at pH values of 4, 6, and 8 [42]. The measured AEC values ranged from 0.60 to 27.8 cmol kg^{-1}. The study carried out by Schell and Jordan on kaolinite, pyrophyllite, halloysite, and bentonite showed that there are close relationships between the anion exchange capacity of these materials and their physicochemical properties [43]. The results showed that materials rich in iron oxide, aluminum, and amorphous silicates exhibited a high anion exchange capacity. Although several investigations have reported the efficiency of laterites as adsorbent materials for the removal of inorganic pollutants, we do not know much about the relationship between the AEC of natural laterites and their efficiency for the removal of anionic pollutants.

Therefore, there is clear evidence that XRPD, FT-IR, SEM, CEC, and AEC analyzes are valuable techniques for evaluating the capabilities of laterites in the adsorption of inorganic and organic pollutants. XRPD analysis studies the determination of mineral phases. FT-IR studies highlight the different vibration bands of mineral phases in the laterites. SEM images evaluate the morphology of the mineral phases. However, very few studies combine these techniques to provide in-depth insights into the potential ability of laterites to adsorb inorganic pollutants from aqueous solution.

This study aims to determine: (i) the physicochemical and structural characteristics of two natural laterites, named KN and LA, by using various techniques, such as XRPD, FTIR, SEM+EDX, DSC, CEC, and AEC; (ii) the correlation between those physicochemical and structural characteristics and the potential usage of the natural laterites as adsorbent materials. This work makes it possible to determine how the physicochemical properties of these natural laterites predispose them to be potential adsorbent materials.

2. Materials and Methods

2.1. Origin of Samples

We collected laterite samples from two distinct sites in Burkina Faso (**Figure 1**). The first one was collected in the Northern part of Kaya, and the second one was collected in Laye. To facilitate the laterite samples designation in the text (**Table 1**), we referenced KN and LA for Kaya North and Laye, respectively. The laterite from KN is light red, and the one from LA is red-brown.

Table 1. Sampling sites and geographical coordinates.

References	Sampling sites	Geographical coordinates		Observation
		North Latitude	West Longitude	

 doi:10.20944/preprints202502.2150.v1

KN	Kaya North	13°07′13.47″	1°06′52.28′′	Light red
LA	Laye	12°31′27.05″	1°47′07.22′′	Red-brown

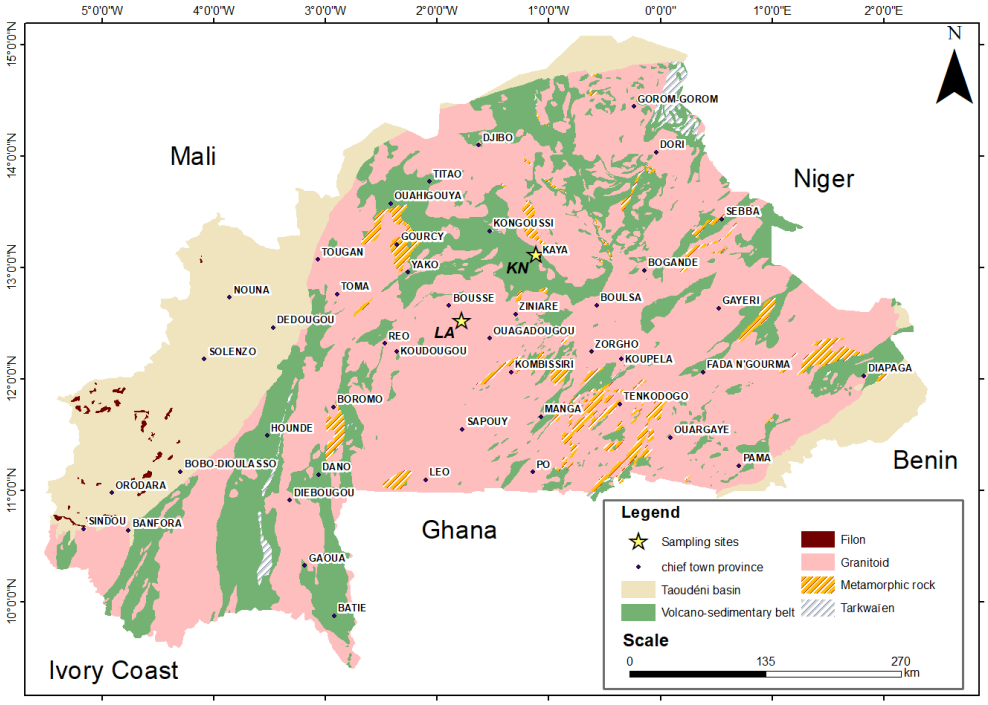

Figure 1. Location of collected laterite samples.

2.2. Specific Geological Contexts of the Sites

The territory of Burkina Faso is divided into square degrees, and each site belongs to a square degree. The geological details of these square degrees are shown on the various positioning maps produced for the different sites.

2.2.1. Geological Context of the Northern Kaya Site

This site belongs to the Kaya square degree, located between latitudes 13° and 14° North and longitudes 1° and 2° West. The geological formations are primarily composed of volcanic and volcano-sedimentary rocks (Figure 2). These rocks form relief areas, while the flat vast regions, at altitudes ranging from 300 to 350 meters, comprises granitic materials such as protoliths. From a geological point of view, the KN samples originate from the environment of Birimian rocks, stemming from andesine (with a calcic-alkaline affinity), basalt, and dacit alteration.

Preprints.org (www.preprints.org) | NOT PEER-REVIEWED | Posted: 27 February 2025 doi:10.20944/preprints202502.2150.v1

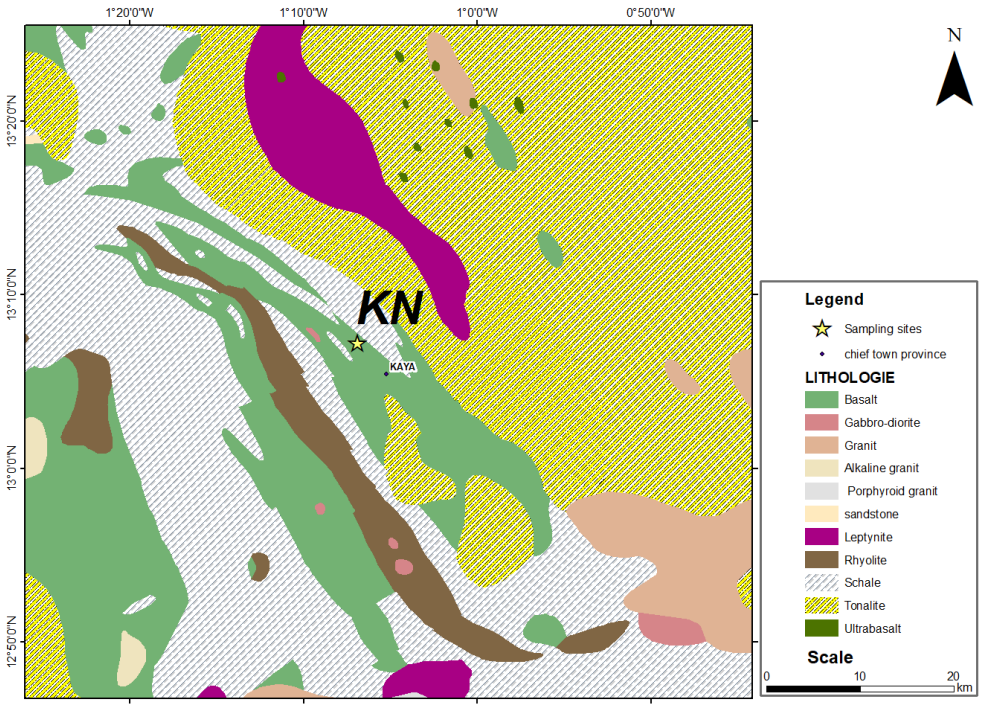

Figure 2. Geological map of the northern Kaya laterite site.

2.2.2. Geological Context of the Laye Site

The Laye (LA) site belongs to the square degree of Ouagadougou and is located at 35 km from Ouagadougou. The square degree of Ouagadougou is located between parallels 12 and 13° North latitude and meridians 1 and 2° West longitude. Unlike Kaya, this square degree is mainly composed of granite formations, corroborating its generally flat relief. The Laye site is located on highly indurated lateritic formations derived from a granitic protolith (alkaline granite). From a geological point of view, this area is located in an environment of Precambrian rocks (Figure 3).

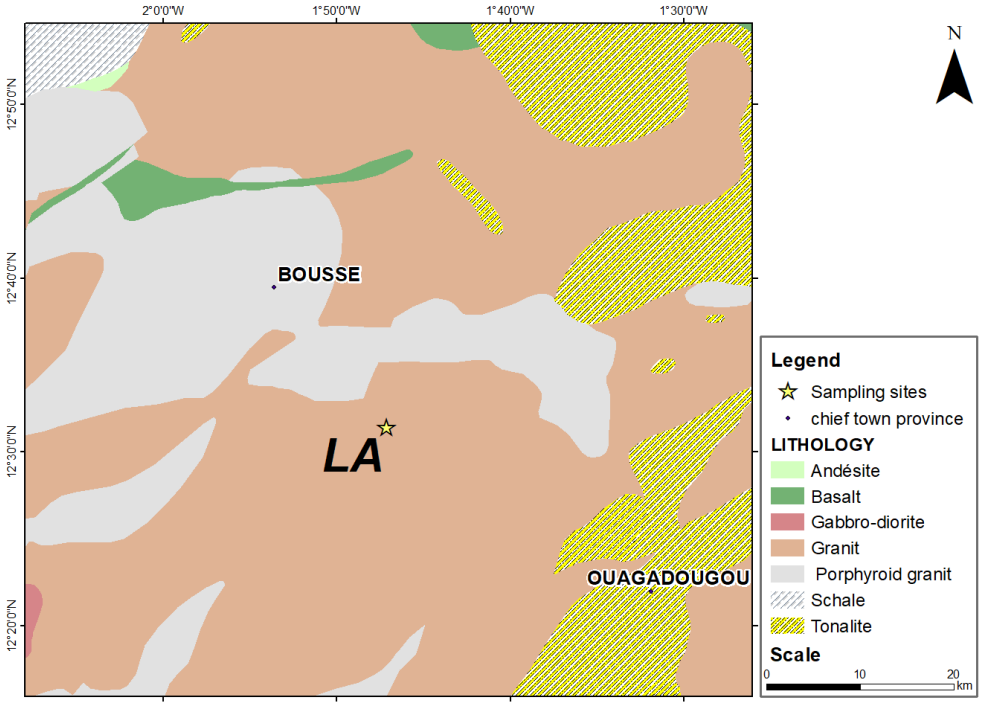

Figure 3. Geological map of the Laye laterite site.

 doi:10.20944/preprints202502.2150.v1

2.3. Raw Materials Characterization

2.3.1. Chemical Composition

Elementary chemical analysis was performed by ICP (ICP- AES-IRIS Intrepid II XSP model). 0.25 g of laterite samples were digested in a microwave oven in 4 mL of HF (30 % w/w), 3 mL of H_2SO_4 (96 % w/w), and 3 mL of HNO_3 (65 % w/w) [44].

2.3.2. Infrared Spectroscopy

Fourier-transform infrared (FTIR) spectroscopy was performed using a Shimadzu FTIR-8400S spectrometer to identify functional groups on the laterite samples. The spectra were acquired by accumulating 20 scans with a resolution of 4 cm^{-1} over a wavelength range of 400 to 4000 cm^{-1}. Infrared analysis of the laterite samples was performed using the potassium bromide pelletizing technique. The pellets were made by mixing 5 mg of each sample with 500 mg of potassium bromide (KBr, Merck, Darmstadt (Germany)). The mixture was finely ground and subjected to a pressure of ten (10) tons. The pellet thus formed was analyzed with a spectrophotometer.

2.3.3. X-ray Powder Diffraction (XRD)

The structure, characteristics, and phase composition of the laterite samples were analyzed by X-ray diffraction analysis (XRD) on a SIEMENS D5000 equipment running with the DIFFRAC AT software version 2.0 (Co-Kα radiation; graphic monochromator; measurement in the 20 to 80 θ game; 40 kV voltage and 30 mA current).

2.3.4. Semi-quantification

The semi-quantitative analysis of the different mineral phases was carried out by coupling the X-ray diffraction results with those of chemical analysis. This coupling allowed for the evaluation of the relative quantities of the minerals contained in the laterites using Equation **1** [2,45].

$$T(a) = \sum M(i) \times P_i(a) \quad (1)$$

T (a): content of the oxide "a" in the sample, Mi: content (%) of mineral "i" in the sample, Pi (a): proportion of oxide "a" in mineral "i" (this proportion is deduced from the ideal formula assigned to mineral "i"). The quantitative approach has been performed on the following basis:

- Alumina is distributed in kaolinite,
- Iron oxide is distributed between Goethite and Hematite,
- Silicon oxide is distributed between Quartz and Kaolinite.

The mass percentages of mineral elements were obtained from Equations 2a-d

$$\%Kaolinite = \%Al_2O_3 \times \frac{M_{Kaolinite}}{M_{Al_2O_3}} \quad (2a)$$

$$\%Quartz = \left(\%SiO_2 - \%Kaolinite \times \frac{M_{SiO_2 \times 2}}{M_{Kaolinite}}\right) \times \frac{M_{Quartz}}{M_{SiO_2}} \quad (2b)$$

$$M_{(Goethite+Hematite)} \rightarrow \%Fe_2O_3$$
$$M_{Goethite} \rightarrow \%Goethite \quad (2c)$$

$$\%Hematie = (\%Al_2O_3 - \%Goethite) \quad (2d)$$

2.3.5. Scanning Electron Microscopy (SEM)

SEM was used to analyze the surface properties and morphology of the raw laterites. Samples were loaded onto a double-sided carbon tape attached to SEM tubs and then coated with gold using a sputter coater to avoid charging effects. SEM images were acquired using a Scanning Electron Microscope (Microspec-WDX 600/OXFORD). The accelerating voltage was 20 kV, which allowed a magnification of up to 30,000X.

2.3.6. Differential Scanning Calorimetry (DSC) and Thermogravimetric Analysis (TGA)

 doi:10.20944/preprints202502.2150.v1

Thermogravimetric and differential scanning calorimetry analysis was carried out on a TGA/DSC thermal analyzer (TGA/DSC1-STARe METTLER TOLEDO System) under a nitrogen atmosphere at a heating rate of 10 °C/min. A mass of 5 g of raw laterite powder with a particle size of 106 µm was heated from 25°C to 1500°C. The TGA/DSC data were analyzed using the METTLER TOLEDO STARe software.

2.3.7. Zeta Potential Measurements

Zeta potential measurements were performed to determine the electrostatic magnitude between particles of laterite samples. Zeta meter equipment (Zetasizer nano ZS Malvern) was used to measure the isoelectric point (IP) of the natural laterite samples. The pH solution was adjusted with 0.025 mol.L^{-1} HCl and 0.025 mol.L−1 NaOH solutions. Data was calculated using the software ZS (Malvern Panalytical).

2.3.8. Specific Surface Area and Porosity by Nitrogen Sorption Analysis

Nitrogen (N_2) sorption isotherms at 77 K were measured using the BelSorp-max instrument running with the Bel Japan Inc Surface Area and Porosity Analyzer. Before N_2 sorption measurements, samples were vacuum-dried at room temperature for at least 24 hours, followed by degassing under heating and vacuum, using a Sample Degas System. The value of each material's specific surface was determined with a device from Bel Sorp-max / Bel Japan.Inc brand controlled by Bel Japan software. Inc.

2.4. Cation Exchange Capacity (CEC)

The cation exchange capacity was determined by shaking 0.5 g of laterite sample with 30 mL of 0.05 mol/L hexaamminecobalt (III) chloride ($[Co(NH_3)_6]^{3+}$, $3Cl^-$) solution for 2 hours. The supernatant was collected and analyzed by SHIMADZU UV-visible spectrometry at 475 nm. The cation exchange capacity was calculated according to Equation 3.

$$C.E.C = \frac{(C_i - C_f) \times V}{m} \times \quad (3)$$

C_i and C_f are the initial and equilibrium concentrations of the hexaamminecobalt (III) chloride solution (mol/L), respectively; m is the mass of the laterite sample, and V is the volume of the solution.

2.5. Anionic Exchange Capacity (AEC)

The anion exchange capacity (AEC) was determined by adapting the method proposed by Zelazny et al. to our study context [46]. It was determined at different pH values (pH framing the isoelectric point of the material) using chloride ions as an anionic index. The AEC measurement methods are based on the same principle as the Cation Exchange Capacity (CEC) and are subject to the same constraints.

Thus, 2 g of laterite was placed in a series of centrifugation tubes with a capacity of 50 mL. Then, 20 mL of $CaCl_2$ (0.1 mol/L) were added and left under gentle stirring for 1 hour to saturate the laterite with chloride. After 1 hour of stirring, the mixtures were centrifuged at 3000 rpm for 5 minutes, and the residues were recovered. The residues were rewashed five times with 20 mL of $CaCl_2$ (0.002 mol/L), left in contact for 1 hour, and centrifuged for 5 minutes at 3000 rpm. Then, 5 mL of $CaCl_2$ (0.002 mol/L), 1.5 mL of HCl (0.1 mol/L), and 3.5 to 5 ml of milli-Q water, respectively, were added so that the total volume was equal to 10 mL.

The suspensions were placed in a bath at 25° C for six days, shaking them manually, thrice daily. On the seventh day, the pH of each suspension was measured, and the mixture was centrifuged at 3000 rpm for 10 minutes. The chloride ions ($\boldsymbol{C_1}$) were then evaluated. The mass of the residues and of the tube was weighed and recorded in order to determine the volume ($\boldsymbol{V_1}$) of the solution that remained trapped.

The residues were resuspended in 30 mL of an ammonium nitrate solution (1 mol.L^{-1}), left in contact for 1 hour, and then centrifuged at 3000 rpm for 10 minutes. The clear solution was recovered

 doi:10.20944/preprints202502.2150.v1

in a 100 mL volumetric flask (V_2). This operation was repeated twice, and the flask's contents were adjusted with an ammonium nitrate solution (1 mol.L^{-1}). The chloride ions ($\boldsymbol{C_2}$) were assayed in this final solution, and the Anion exchange capacity was determined by Equation **4**:

$$\text{AEC}\ (\text{cmol.kg}^{-1}) = (C_2V_2 - C_1V_1) \times \frac{0.1 \times z}{M \times W} \quad (4)$$

Where:

C_1: concentration ($mg.L^{-1}$) of Cl^- in final washing solution of 0.1 M $CaCl_2$;

C_2: concentration ($mg.L^{-1}$) of Cl^- in the displacing solution of 1 M NH_4NO_3;

V_1: volume (mL) of the solution contained in laterites after the final washing of 0.1 M $CaCl_2$;

V_2: total volume (mL) of the displacing solution 1 M NH_4NO_3;

M and z: are atomic weight and charge of Cl^- respectively;

W: laterite sample weight (g).

3. Results and Discussion

3.1. Chemical Composition

The chemical composition in **Table 2** indicates the major oxides (SiO_2, Al_2O_3, and Fe_2O_3) and the minor oxides (Na_2O, K_2O, and TiO_2) in KN and LA samples. Other properties, such as apparent density, total organic carbon (TOC), and organic matter (OM), are also shown in **Table 2.**

Table 2. Physico-characterization and chemical analyzes of KN and LA laterite samples.

Properties	KN	LA
Total organic carbon (TOC) (%)	0.16	0.09
Organic matter (OM) (%)	0.73	1.32
Inorganic composition (wt.%)		
Fe_2O_3	20.8	17.65
Al_2O_3	14.09	6.74
SiO_2	50.16	53.70
K_2O	1.70	1.82
Na_2O	1.43	1.40
TiO_2	2.10	2.10
MgO; MnO_2; BaO; CaO; Cr_2O_3; B_2O_3; Ga_2O_3	traces	traces
L.O.I	11.5	10.4

L.O.I: loss on ignition.

According to the literature [13,32], iron is found as oxyhydroxides. Oxides of potassium, sodium, and titanium are in small amounts in all two samples. These results suggest that quartz, aluminosilicates, and iron minerals are predominant in the samples studied. The low levels of potassium, sodium, and titanium oxides indicate that compounds containing titanium, potassium, and sodium are non-existent or present in tiny proportions. The elements in KN and LA are grouped according to their family in **Table 3**.

Table 3. Chemical composition of the samples by type of elements in % by weight.

Family	Alkalis	Alkaline-earth	Metals	Silica
KN	3.1	0.1	37.3	50.2
LA	3.2	0.2	26.6	53.7

This study is the first to carry out this classification by type of elements, providing useful criteria of the elements present in lateritic materials that can influence the adsorption of inorganic pollutants in solution.

3.2. Specific Surface Area and Porosity using Nitrogen Sorption Analysis

 doi:10.20944/preprints202502.2150.v1

Figure 4 shows the N_2 adsorption–desorption isotherms of the raw laterite samples. The initial part of the isotherms for all laterites of a type I shape (IUPAC classification) indicates the presence of micro pores [47]. As determined by the B.E.T method from **Figure 2**, the specific surface values are 58.65 m^2/g and 41.15 m^2/g for KN and LA samples, respectively. These specific surface area values are significantly high when compared to values reported in the literature for natural laterites in the range of 16 – 32 m^2/g [15,17,22,35,37,38].

Table 4 shows the specific surface area values by B.E.T and the pores volume of the two samples, as well as the literature-reported values of specific areas of other laterites.

Table 4. Comparison of the B.E.T specific surface area and pore volume values of the two laterites with other laterites in the literature.

Laterites	Specific surface area by B.E.T (m^2/g)	Pore volume (cm^3/g)	References
Laterite raw (India)	15.3	0.013	[15]
Red soil	16.1	-	[48]
Laterite raw (India)	17.5-18.5	0.011	[35]
Modified laterite	178-184	0.22	[35]
Laterite raw (Vietnam)	10.9	0.01	[49]
Laterite raw	24.7	0.08	[37]
Iron rich laterite	32	-	[38]
Calcined laterite	187.5	0.04	[50]
Laterite soil (DA)	35.08	0.10	[51]
Laterite soil (KN)	58.6	0.14	This study
Laterite soil (LA)	41.1	0.10	

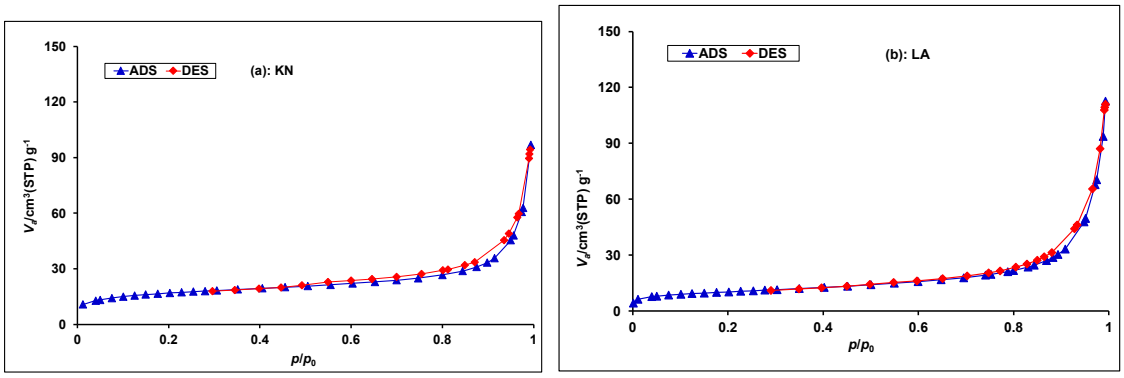

(a) (b)

Figure 4. N_2 adsorption/desorption isotherms of (a) KN and (b) LA.

We noted that our investigated lateritic materials showed high specific surface area values compared with most natural materials reported in the literature used to remove inorganic pollutants. These particular surface areas suggest that the natural materials we investigated are potential candidates for the adsorption of inorganic pollutants in solution. Several authors have highlighted the importance of having high specific surface area values in their studies using clay and/or lateritic materials to remove inorganic pollutants [50–53].

3.3. Determination of the Anionic Exchange Capacity (AEC)

The anionic exchange capacity values (**Table 5**) of the measured laterites ranged from 86.50 ± 3.40 to 73.91 ± 9.94 cmol(-).kg^{-1} and 73.59 ± 3.02 to 64.56 ± 4.08 cmol(-).kg^{-1}, respectively. The anionic exchange capacity of laterites increased with the decreasing pH of the solution. This significant increase in AEC with decreasing pH is due to positive charges that are located on iron hydroxides

 doi:10.20944/preprints202502.2150.v1

associated with aluminum. The high values of the anion exchange capacities of the investigated laterites would be an asset for using them as adsorbents to remove anionic pollutants.

The results obtained are similar to other materials studied in the literature. Cheng et al. determined the anion exchange capacity of black carbon at pH 7.1 and 3.4 and obtained values of 84 and 18 cmol.kg-1, respectively [54]. Lawrinenko et al. also determined the anion exchange capacity of biochar produced from three raw materials at 500 and 700° C at pH 4, 6, 8 [42]. The measured AEC values ranged from 0.60 to 27.8 cmol (-). kg^{-1}. Moreover, the study by Schell and Jordan [43] on kaolinite, pyrophyllite, halloysite, and bentonite materials showed that there are close relationships between the anion exchange capacity of these materials and their physicochemical properties. Indeed, materials rich in iron oxide, aluminum oxide, and amorphous silicates showed a high anion exchange capacity. Consequently, the investigated natural laterites containing important amounts of iron oxide and alumina are likely to exhibit high anion exchange capacity values, which gives them interesting adsorbent properties.

Table 5. Anionic exchange capacity of laterites.

Laterite KN		Laterite LA	
pH	**AEC (cmol(-).Kg^{-1})**	**pH**	**AEC (cmol(-).Kg^{-1})**
3.47 ± 0.02	86.50 ± 3.40	3.67 ± 0.04	73.59 ± 3.02
3.67 ± 0.01	86.02 ± 8.29	3.84 ± 0.04	73.33 ± 3.03
5.51 ± 0.05	73.91 ± 9.94	5.22 ± 0.04	64.56 ± 4.08

3.4. Determination of the Cation Exchange Capacity (CEC)

The CEC value, determined using the hexaamminecobalt (III) chloride method, is an important parameter in assessing the adsorption capacity of adsorbent materials for cations removal [18]. We found high CEC values in the order of 52.3 ± 2.3 and 58.7 ± 3.4 cmol(+)/Kg (dried matter) for KN and LA samples, respectively. We cannot compare these results with previous literature data because we did not find extensive documentation of this parameter for natural laterites that remove inorganic pollutants from solution. To our knowledge, our study appears to be the first to provide scientific documentation of this parameter for laterites used in the field of adsorption of inorganic pollutants. However, we compare the CEC values obtained in this study with other adsorbents in **Table 6 below**. These specific surface area values are significantly high when compared to values reported in the literature for other natural laterites. We noted that the CEC values of the KN and LA laterites samples are comparable with those reported for other natural adsorbents. Considering the CEC and the specific surface area values, compared with literature values on natural adsorbents, these materials could be considered potential candidates for heavy metal cation removals through adsorption processes [55,56].

The laterites of Burkina are rich in iron oxide and alumina, like the laterites of other countries used to eliminate heavy metals and/or metalloids in ground waters [35–37]. Considering all of these physical and chemical characteristics, we can conclude that the natural laterites of Burkina Faso prove to be potential candidates for the adsorption of heavy metals and/or metalloids in groundwater.

Table 6. Comparison of CEC values for KN and LA laterites with others adsorbents.

Adsorbents	C.E.C (cmol(+)/kg)	References
Clay mineral	42.38	[33]
Peat soil	33-48	[57]
Bauxite	24-33	[57]
Iron concretion	59-65	[57]
Natural clay	18.66	[58]
Kaolinite	13.00	[59]
Bentonitic clay	67.00	[60]
Ivory Coast clay	35.47	[61]

 doi:10.20944/preprints202502.2150.v1

Laterite soil (KN)	52.33	This study
Laterite soil (LA)	58.70	

3.5. Isoelectric Point (IP) of Laterite Samples

Figure 5 shows variations of zeta potential versus pH of laterite sample solutions. These variations allowed the determination of isoelectric points (IP). For zeta potentials whose values equal zero, IP values are 3.82 and 3.78 for KN and LA samples, respectively. According to the literature [62], the theoretical value of IP, calculated based on the silica and alumina percentage, is approximatively 4.6. The experimental values of IP are not far from the theoretical value. The observed deviations are the result of the iron percentage higher than the one of alumina and also by the presence of other oxides in the samples.

The values of the isoelectric point (IP) of laterites, KN (3.82) and LA (3.78), mean that the surfaces of these laterites are positively charged at pH levels below these values, which favors the adsorption of anionic pollutants. The increase in adsorption below IP is due to electrostatic attraction between the positive surface and the negative charge of the anions. Similarly, the decrease in adsorption with increasing pH is due to electrostatic repulsion between the opposing surface and the negative charge of anions. The electric surface charge plays an important role in the adsorption of inorganic pollutants on laterites.

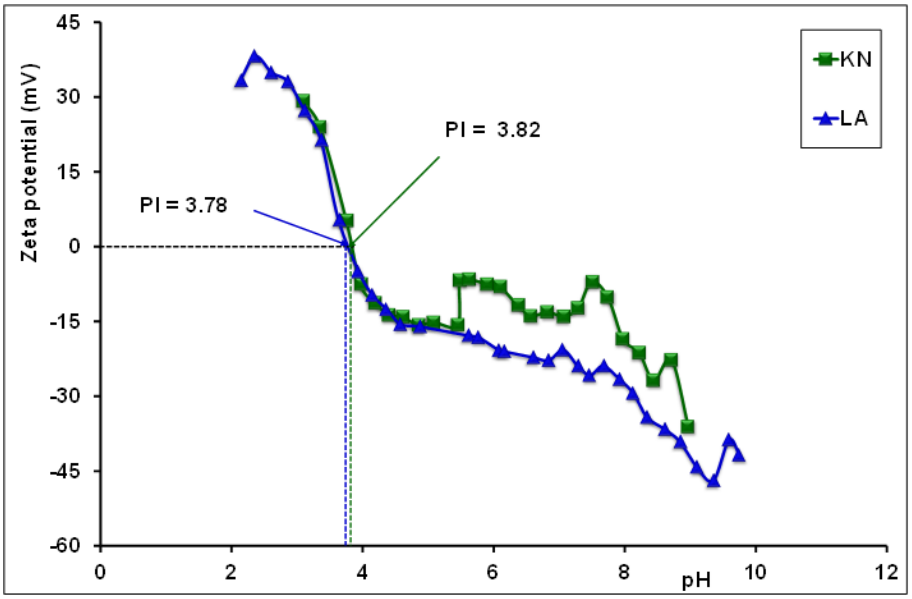

Figure 5. Isoelectric point of laterite soils determined from variations of zeta potential versus pH.

3.6. Mineralogical Characterization

3.6.1. X-Ray Diffraction (XRD)

Figure 6 shows the XRD pattern. The major mineral phases of the two laterite samples KN and LA include quartz (SiO_2), kaolinite ($Al_2Si_2O_5(OH)_4$), hematite (Fe_2O_3), and goethite ($FeO(OH)$). These mineral phases are those commonly found in laterites [13,63]. The minerals present in KN and LA laterites were compared with other laterites presented in the literature and used for the adsorption of heavy metals and/or metalloids (**Table 7**).

Several authors [8,24–26] who have used laterites to adsorb inorganic pollutants suggested that these laterites should be rich mainly in hematite, goethite, or aluminum oxides.

Table 7. Comparison of the main minerals present in KN and LA laterites with other natural laterites reported in the literature.

 doi:10.20944/preprints202502.2150.v1

Samples	Main minerals	References
red soil	quartz, hematite, goethite, aluminum oxides	[48]
raw laterite	quartz, hematite, goethite, aluminum oxides, iron oxides, titanium oxides	[22,35,37]
iron-rich laterite	quartz, hematite, goethite, aluminum oxides	[38]
laterite (Australia)	quartz, hematite, goethite, aluminum oxides	[64]
DA	quartz, hematite, goethite, aluminum oxides	[2]
laterite KN	quartz, hematite, goethite, aluminum oxides	This study
laterite LA	quartz, hematite, goethite, aluminum oxides	

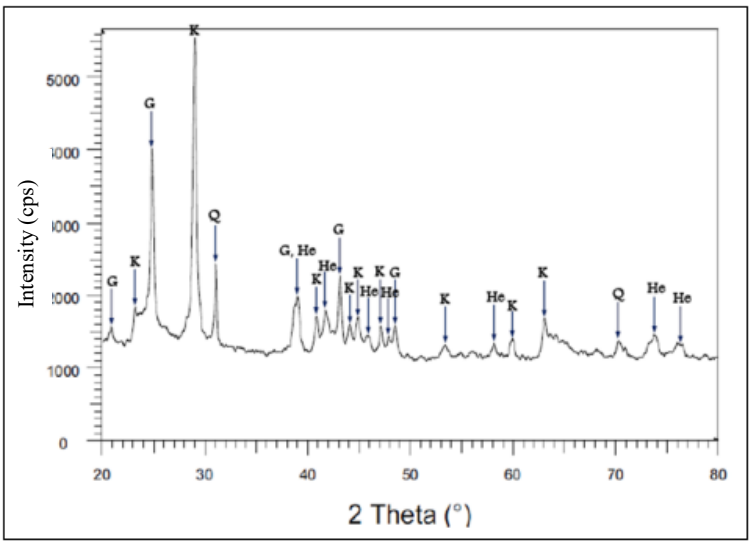

(a)

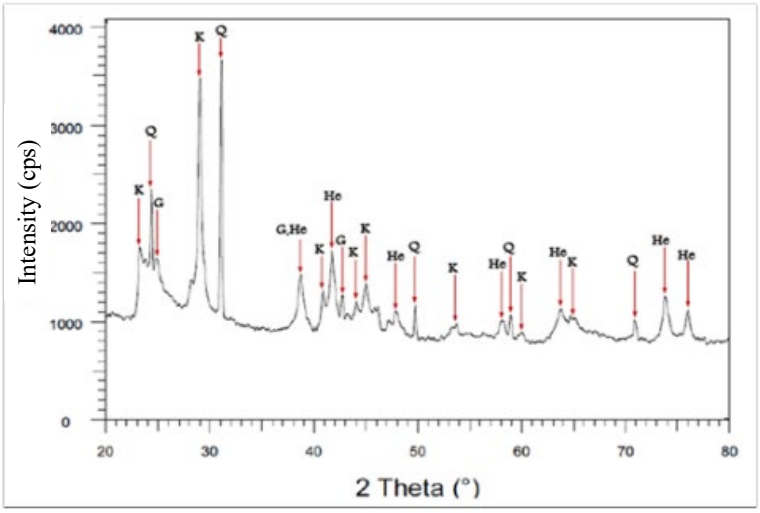

(b)

Figure 6. X-Ray diffraction pattern of laterite samples: (a) KN sample; (b): LA sample. K = kaolinite, Q = quartz, He = hematite et G = goethite.

3.6.2. Infrared Spectrometry (IR)

 doi:10.20944/preprints202502.2150.v1

Figure 7 shows the FT-IR spectra of laterite samples. The FT-IR spectrum could distinguish three spectral domains: 3700 - 3400 cm-1, 1650 - 900 cm-1, and 800 - 400 cm-1, respectively. **Table 8** gives the different attributions of the observed bands.

Table 8. Assignments of FT-IR bands of KN and LA laterite samples.

(*ν* en cm^{-1})	Probable bands assignments	References
3695	Vibration bands linked to external hydroxyls (Al-OH) in kaolinite	[65]
3618	Vibration bands related to internal hydroxyls (Al-OH) in kaolinite, located between a tetrahedron sheet and an octahedron $Al_2(OH)_6$	[65]
3170	Band related to –OH bound vibrations in goethite	[31]
3430	Band related to water contained in the intersheet	[65]
1638	Band related to hygroscopic water	[65,66]
1112	Vibration band corresponding to Si-O bound of kaolinite	[28,29,65]
1034	Vibrations bands corresponding to Si-O bound of kaolinite and Fe-OH bound of goethite	[29,30,65]
1004	Vibrations bands related to OH bounds of kaolinite and Fe-OH bound of goethite	[29,30]
914	Band related to distortion vibrations of Al-OH bound of kaolinite and Fe-OH bound of goethite	[29,30,65]
791	Band corresponding to bending vibration of Si-O and Fe-OH bounds of kaolinite	[28,31]
752	Vibrations bands related to OH bounds of kaolinite and Fe-OH bound of goethite	[30,65]
694	Vibrations bands related to OH bound of kaolinite and Si-O bounds of quartz	[31]
539	Bands corresponding to distortions vibrations of Si-O-Al bound of kaolinite and Fe-O bound of hematite	[29,31,65]
470	Vibrations bands related to flexion of Si-O-Si and Fe-O bounds of hematite	[28,31]
421	Vibrations bands of Si-O-Si bounds of kaolinite	[29]

The results of the infrared spectrum analysis confirm the presence of mineral phases, such as goethite, hematite, quartz, and kaolinite, which we had already identified during the previous X-ray diffractogram analysis.

Preprints.org (www.preprints.org) | NOT PEER-REVIEWED | Posted: 27 February 2025 doi:10.20944/preprints202502.2150.v1

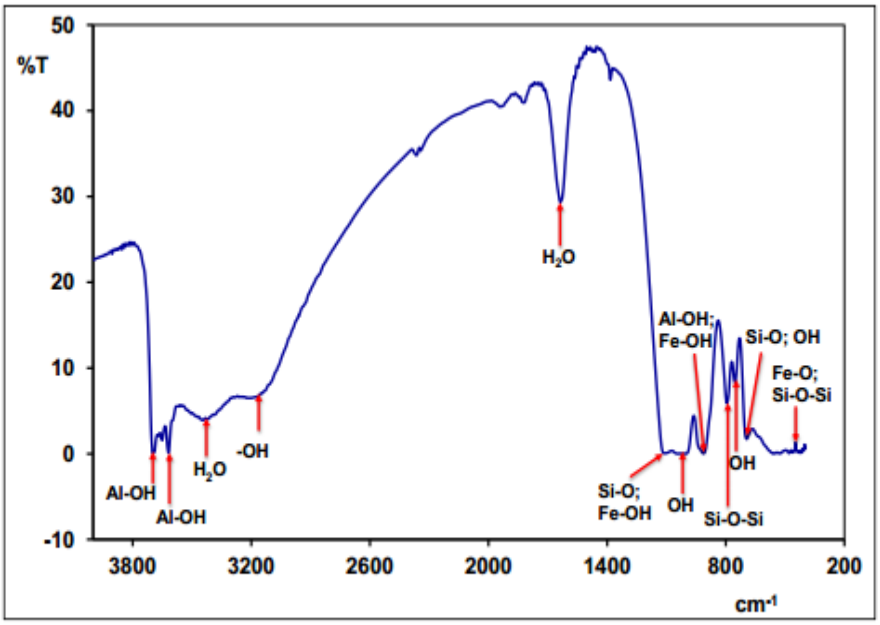

(a)

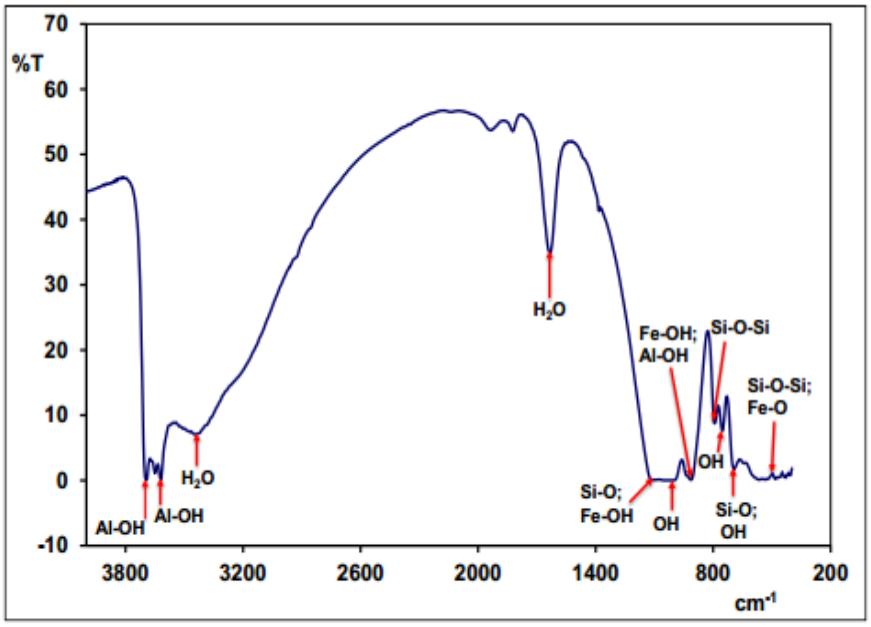

(b)

Figure 7. FT-IR spectrum of natural laterites: (a). KN sample; (b). LA sample.

3.6.3. Semi-Quantification

Table 9 shows the results of the semi-quantitative analysis of the different mineral phases present in the KN and LA laterites. These results show that the laterites are composed of hematite (13.36% to 11.43%), goethite (7.44% to 6.31%), kaolinite (35.64% to 17.05%), and quartz (33.58% to 45.77%).

Table 9. Mineralogical composition of laterites in % by mass.

Mineral phases	Hematite	Goethite	Kaolinite	Quartz

 doi:10.20944/preprints202502.2150.v1

	KN	13.36	7.44	35.64	33.58
wt (%)	LA	11.43	6.31	17.05	45.77
	DA*	13.11	7.29	48.32	22.53

*DA: our previous work on a natural laterite (See Reference [2]).

The results from the chemical, mineralogical, cation exchange capacity, and anion exchange capacity analyzes lead to the conclusion that the natural laterites investigated possess good adsorbent characteristics for removing inorganic and organic pollutants from aqueous matrices.

3.7. Thermogravimetric Analysis and Differential Scanning Calorimetry (TGA /DSC)

DSC/TGA techniques provide information on the thermal stability and phase transformations of lateritic materials. **Figure 8** shows experimental TGA/DSC curves of KN and LA samples. Several thermal processes are observed. The endothermic peak located between 94°C to 110°C in the DSC curves is related to hygroscopic water loss or hydration in the samples. This incident is associated with 1% and 1.5% weight loss in the TGA curves for KN and LA samples, respectively. Endothermic peaks between 296 °C and 356 °C, followed by 4.1 % and 1.3% weight losses for KN and LA, respectively, are due to goethite transformation in hematite (**Equation 5**).

$$2\alpha - FeOOH \longrightarrow \alpha - Fe_2O_3 + H_2O \quad (5)$$

Endothermic peaks between 500 °C and 600 °C in the DSC curves are assigned to kaolinite deshydroxylation (**Equation 6**), indicating 7.3 % and 8.7% weight losses in the TGA curves for KN and LA, respectively. It is suggested that structural hydroxyls are removed during the chemical reaction, leading to the destruction of the mineral crystalline network. As for kaolinite, deshydroxylation forms an amorphous phase which is named metakaolinite [67,68].

$$Si_2O_5Al_2(OH)_4 \rightarrow 2SiO_2 - Al_2O_3 + 2H_2O \quad (6)$$

The only exothermal peaks observed in the DSC curves are located between 950°C and 1000°C. These peaks may be attributed to the structural reorganization of metakaolinite in spinel phase and amorphous silica (**Equation 7**) [65,67].

$$2[2SiO_2 - Al_2O_3] \rightarrow Si_3Al_4O_{12} + SiO_2 \quad (7)$$

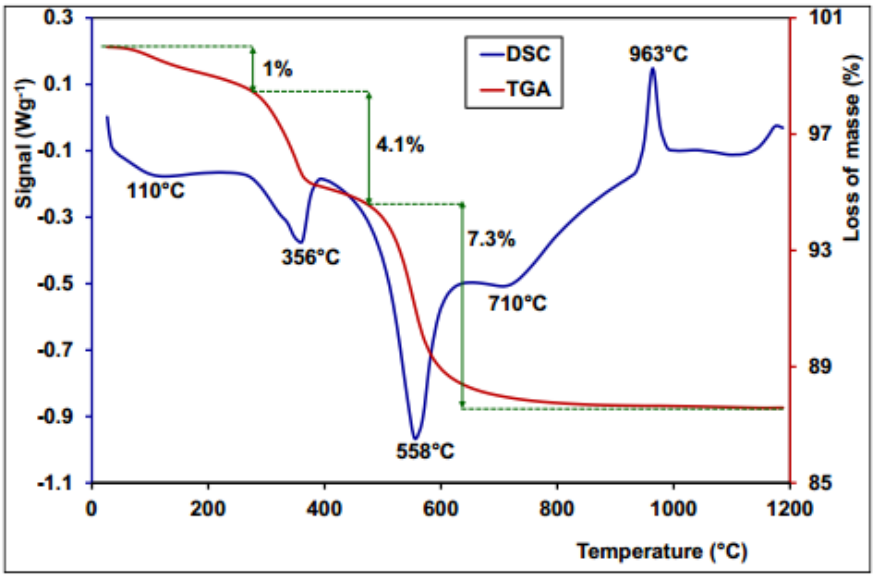

(a)

 doi:10.20944/preprints202502.2150.v1

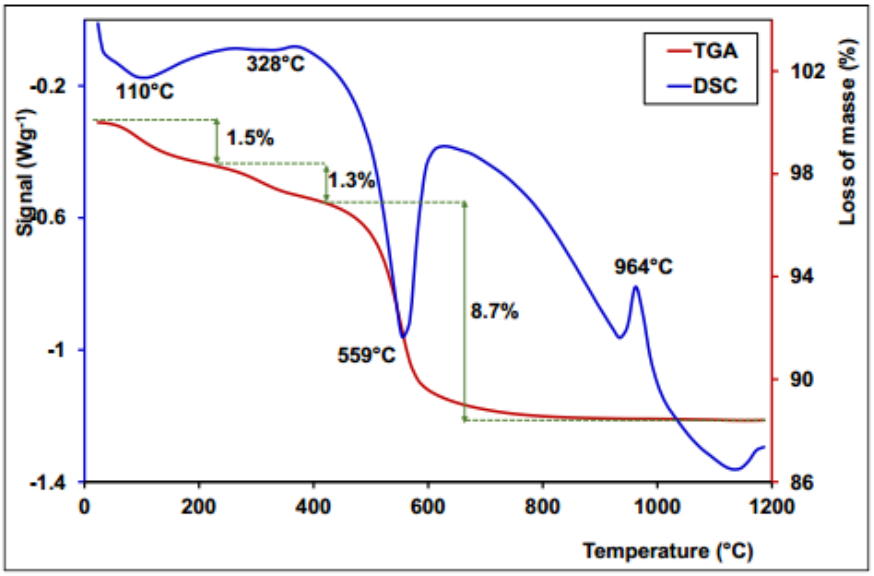

(b)

Figure 8. TGA/DSC curves of the lateritic samples: (a). KN sample; (b). LA sample.

DSC/TGA results can indicate changes in the pore structure, influencing the available adsorption sites. DSC analyses reveal the stability of the mineral phases present in laterites. A stable phase is generally more effective at adsorbing anionic and/or cationic pollutants. Temperature variations can affect interactions between laterites and adsorbed molecules. DSC and TGA are essential for understanding the physical and chemical properties of materials, which may include their ability to adsorb contaminants such as heavy metals.

3.8. Microstructural Characterization

Figure 9 shows the scanning electron microscopic images of KN and LA samples at a scale ranging from 1 to 5 µm. The samples exhibit agglomerated particles whose size reaches several hundred nanometers. Moreover, some plates with irregular sizes could be seen in the samples. Such results are characteristic of kaolinite mineral phases as previously described in the literature [33].

The complex porous structures of laterites, especially mesopores, play a crucial role in the adsorption of inorganic pollutants, facilitating physical and chemical interactions with dissolved species [53]. The distribution of the different types of pores (Mesopores and/or Micropores) in the laterite determines its adsorption capacity and affinity for different types of inorganic pollutants. Laterite with a wide range of pore sizes will generally be more effective for adsorbing various pollutants of various sizes.

 doi:10.20944/preprints202502.2150.v1

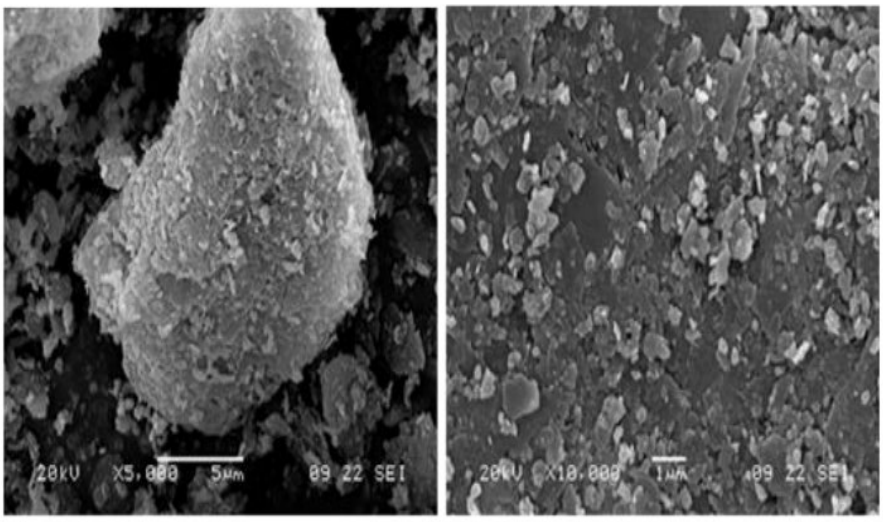

(a)

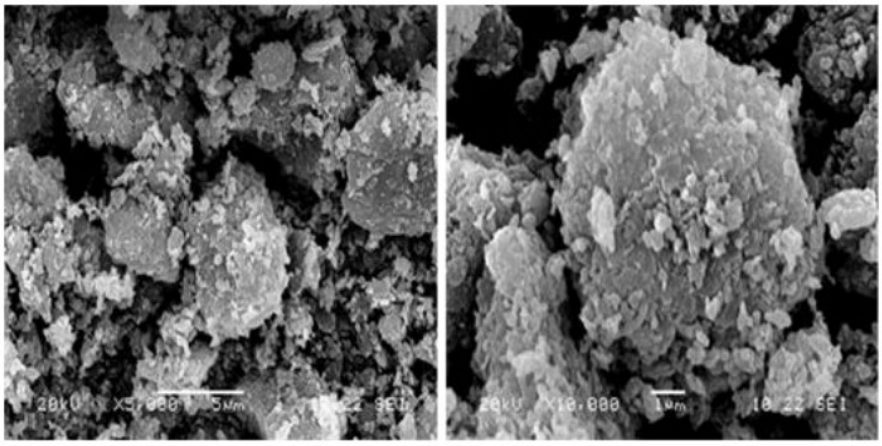

(b)

Figure 9. Scanning electron microscopic images of: (a). KN sample; (b). LA sample.

3.9. Comparison of the Main Physicochemical Properties Related to the Adsorption of Laterites from Burkina Faso with Those Reported in the Literature

This study investigated the main physicochemical properties of two laterites (LA and KN) from Burkina Faso, showing how to link these properties to an adsorption process. The results showed that these laterites possess interesting properties, allowing their use to treat water contaminated by anionic and/or cationic pollutants. We compared the physicochemical properties of the two laterites with regard to their adsorption properties with other reported literature results regarding laterites used for the adsorption of anionic and/or cationic pollutants. **Table 10** gives the main observations of this comparison. From the results of **Table 10**, we noted that the CEC and AEC determinations are omitted in most studies dealing with the removal of cationic and/or anionic pollutants from aqueous solutions. However, these parameters are crucial to elucidate the adsorption mechanisms, in terms, for example, of surface complexation (inner-sphere and outer sphere surface complexation). Whereas CEC value is an important parameter to determine the adsorption of heavy metal cations, AEC values are more indicated for adsorbents like As(III) and As(V), which appear in solution as neutral or anionic charged species.

 doi:10.20944/preprints202502.2150.v1

Table 10 shows that our study is the first to provide a complete description of laterite properties, in terms of specific surface area, pore volume, DSC/TGA, PZC, chemical composition*, mineralogical characterization*, cation exchange capacity (CEC), and anion exchange capacity (AEC), in relation to the adsorption ability of the material. Indeed, these properties are helpful criteria that provide strong evidence of the adsorption capacity of the laterites regarding the removal of cationic and/or anionic pollutants from aqueous solutions [18–20,43].

Table 10. Comparison of the physicochemical properties of several laterites in relation to pollutant adsorption.

Adsorbent	Adsorbats	AEC cmol (-)/Kg)	C.E.C cmol(+)/kg)	Specific surface area (B.E.T) (m^2/g)	Pore volume (cm^3/g)	DSC /TGA	IEP or PZC	References
Laterite soil	cationic dye	-	-	66.97	-	-	6.6	[69]
Raw laterite	arsenic and fluoride	-	-	31.6037	0.0097	-	-	[70]
Raw laterite	Phosphate	-	-	29.54	0.0676	-	-	[7]
Laterite	Arsenic	-	-	155	0.5489	-	7.1	[8]
Laterite clay	Ni(II) and Co(II)	-	-	17.441	0.005	-	-	[23]
Laterite soil	Arsenic	-	-	15.365	0.013	-	6.96	[15]
Natural laterite	Arsenic	-	-	18.05	-	-	7.49	[16]
Treated laterite	Led	-	-	75.5	0.02	-	6.0	[71]
Plateau laterite ceramic	Pb, Cd, Hg, As, Cu and Cr	-	-	26.73	0.15	-	-	[72]
Limonitic laterite	Pb(II) and Cd(II)	-	-	62.73	0.62	-	-	[24]
Lateritic nickel	Pb(II)	-	-	68.39	-	-	6.70	[26]
Laterite soil	Pb(II) and Cr(VI)	-	-	23.015	0.011	-	-	[25]
Laterite DA**	As(III,V)	40.61-230.80	-	35.08	0.10	-	4.75	[2,51]
Laterite LA	As(III,V)	64.56-73.59	58.7 ± 3.4	58.80	0.14	Det***	3.78	This study
Laterite KN	As(III,V)	73.90-86.50	52.3 ± 2.3	41.10	0.10	Det***	3.82	

*Chemical composition and mineralogical characterization of laterites are common characteristics provided in most studies (See **Table 7**); ** References [2,51] describe our previous study on a natural laterite; Det***: determined.

It is worth noting that the adsorptive properties of laterites are closely related to the geology of the deposit ore they originate from. Indeed, for a naturally occurring laterite ore, the type of parent rock it originates from determines its chemical composition, particularly the percentages of iron,

 doi:10.20944/preprints202502.2150.v1

aluminum, silica, and titanium oxides, as well as its mineralogical composition. The mineralogical composition is generally characterized by mineral phases such as goethite, hematite, and kaolinite. However, laterite ores possess a large variability in their composition. Consequently, even if different geological environments are qualitatively characterized by the same chemical and mineralogical composition, the percentage of oxides can be different from one site to another. The physicochemical properties may also vary. In these circumstances, it is appropriate to focus on quantitative criteria that we need to forecast the ability of the material to remove pollutants in the adsorption process. Moreover, the extent of these criteria may lead to different adsorption capacities. As we have already stated, these critical criteria are the following: specific surface area, pore volume, PZC or IEP, cation exchange capacity (CEC), and anion exchange capacity (AEC).

Here, we compare the results obtained for the three laterites DA, LA, and KN, which we investigated in our laboratory (**Table 11**). KN and LA are described in this study, whereas the DA laterite results are from references [2,51].

The laterites LA and KN in this study are from two sites of different geological environments (**Table 11**). The first site is an environment of Birimian rocks, resulting from the weathering of andesite (with a calcic-alkaline affinity), basalt, and dacit. On the other hand, the second site is a weathering site of alkaline granites located in a Precambrian rock environment. Preliminary investigations showed (**Table 11**) that the removal percentage for arsenic (III) removal at a concentration of 5 mg/L and an adsorbent dose of 15 g/L leads to arsenic (III) removal of 80 ± 0.15% and 98 ± 0.05% for the LA and KN samples, respectively [73]. As for arsenic (V), the removal efficiency was 99 ± 0.02 % for the two samples, KN and LA, at an adsorbent dose of 15 g/L [73]. The laterite DA originates from a well-indurated lateritic plateau that results from the weathering of neutral basic rock [2]. An elimination rate (**Table 11**) of 99.69% for As(V) and 97.30% for As(III) was observed, also for a dose of 15 g/L of laterite [2]. Although the three laterites (LA, KN, and DA) do not have the same geological environments, they showed a high efficiency for arsenic removal due to the combination of their AEC, specific surface area, and pore volume values. In addition, their low IEP or PZC values also favored the adsorption of neutral or anionic-charged arsenic species. Adsorption of arsenic will only be important when the charges on the laterites become positive, which happens at low soil solution pH where anionic-charged arsenic species occur [2,51]. Noting that the surfaces of the samples are positively charged under their PZC values, it is clear these materials better adsorb arsenate (V) anions at pH values under their PZC values. It is, therefore, important to measure the anion exchange capacity (AEC) of the laterites rather than the CEC when we are dealing with the adsorption of neutral or anionic-charged arsenic species.

At this step, the geological environment cannot constitute the sole criterion that would justify the adsorption capacity of negatively charged arsenic species. This criterion may not be decisive in predicting the adsorption capacity of laterite. It must be associated with the physicochemical properties of the laterites. **Table 11** outlines the criteria that affect the adsorptive properties of laterites (LA, KN, DA) in connection with their physico-chemical and geological characteristics.

So far, we have demonstrated that when particular geological environments, such as the Birimian/Precambrian and lateritic plateau environments, are combined with appropriate physicochemical properties, we can expect the lateritic material to be a potential adsorbent (**Table 11**). Unfortunately, in the literature, no direct link has yet been established on this subject. Our study constitutes a preliminary finding, which we will validate by extending our investigations to other lateritic sites in Burkina Faso.

Table 11. Adsorptive properties of laterites used for As(III, V) removal in relation to their physico-chemical characteristics.

Laterite	Geological environment	Mineralogical	AEC cmol (-)/Kg)	Specific surface area	Pore volume (cm^3/g)	IEP or PZC	Efficiency (%)

 doi:10.20944/preprints202502.2150.v1

		Characterizations XRD, FT-IR	(B.E.T) (m^2/g)			
KN	Environment of Birimian rocks, resulting from the weathering of andesite (with a calcic-alkaline affinity), basalt, and dacit.	Det*	73.90-86.50	58.80	0.14	3.82	98 ± 0.05% for As(III) 99 ± 0.02 % for As(V)
LA	Environment of precambrian rocks and alteration of alkaline granites	Det*	64.56-73.59	41.10	0.10	3.78	80 ± 0.15% for As(III) 99 ± 0.02 % for As(V)
DA	Lateritic plateau, well indurated and resulting from the alteration of a neutral basic rock	Det*	40.61-230.80	35.08	0.10	4.75	99.69% for As(V)) 97.30% for As(III)

Det*: determined (**Tables 7 and 8**).

4. Conclusions

We carried out physicochemical analyses and mineralogy of two laterites from Burkina Faso. We determined the properties of these two natural laterites of Burkina Faso with regard to their ability to adsorb heavy metals and/or metalloids from aqueous solutions. These laterite samples were characterized using several physical and chemical techniques, including XRD, FTIR, elementary chemical analyzes, and SEM. The results obtained by X-ray diffraction analysis coupled with infrared showed that the laterites are composed of hematite (13.36% to 11.43%), goethite (7.44% to 6.31%), kaolinite (35.64% to 17.05%) and quartz (33.58% to 45.77%). Chemical analysis showed that these natural laterites are rich in iron and aluminum oxide. The specific surface areas and cation exchange capacity values, as determined by the BET and cobalt hexamine chloride methods, were shown to have suitable values compared to previously determined values in the literature. The anionic exchange capacity of laterites KN and LA ranged from 86.50 ± 3.40 to 73.91 ± 9.94 $cmol(-).kg^{-1}$ and from 73.59 ± 3.02 to 64.56 ± 4.08 $cmol(-).kg^{-1}$, respectively. Furthermore, the investigations on these laterite samples showed they could remove heavy metals and/or metalloids from contaminated ground waters. The main minerals identified in these two Burkina Faso laterites were consistent with those described in the literature. Our investigations lead to some valuable criteria we can base on to classify natural laterites as potential adsorbent materials for the removal of inorganic and/or organic pollutants from aqueous matrices. We showed how the geological environment determined the mineralogical characteristics of the laterites and their chemical composition. Combining the geological environment with appropriate criteria related to the physicochemical properties of the materials opens up interesting perspectives regarding the rapid valorization of the laterites in Burkina Faso as potential adsorbents.

Author Contributions: Conceptualization, C.B, A.L.H and B.G; methodology, C.B, L.C and A.L.H; software, C.B; validation, C.B and L.C; formal Analysis, C.B; investigation, C.B; resources, L.C, A.L.H and B.G; data curation; C.B, L.C; A.L.H and B.G; writing—Original draft Preparation, C.B; Writing—Review and Editing, C.B, L.C, A.L.H, B.G; visualization, C.B and A.L.H; supervision, B.G and A.L.H; project administration; A.L.H and B.G; Funding Acquisition, B.G, A.L.H. All authors have read and agreed to the published version of the manuscript.

 doi:10.20944/preprints202502.2150.v1

Funding: The authors thank the ARES-CCD (Belgium), and the International Science Program (ISP, Uppsala, Sweden) for providing financial support.

Data Availability Statement: All data generated or analyzed during this study are included in this published article.

Acknowledgments: The authors thank the ARES-CCD/PIC project (Belgium), and the International Science Program (ISP, Uppsala, Sweden) for financial support, and the following services for their assistance: the departments of materials science, of metallurgy, and of thermodynamic and physical mathematics of UMONS and Materia Nova Research Center (Belgium).

Conflicts of Interest: The authors declare no conflicts of interest regarding the publication of this paper

References

1. Ndiaye, M.; Magnan, J. P.; Cissé, I. K. and Cissé, L. "Étude de l'amélioration de latérites du Sénégal par ajout de sable," Bull. des Lab. des Ponts Chaussees, **2013**, 280, 123–137.
2. Ouedraogo, R. D.; Bakouan, C.; Sorgho, B.; Guel, B. and Bonou, L. D. "Characterization of a natural laterite of Burkina Faso for the elimination of arsenic (III) and arsenic (V) in groundwater," Int. J. Biol. Chem. Sci., **2019**, 13, 2959–2977. doi: 10.4314/ijbcs.v13i6.41.
3. Najar, M.; Sakhare, V.; Karn, A.; Chaddha, M. and Agnihotri, A. "A study on the impact of material synergy in geopolymer adobe: Emphasis on utilizing overburden laterite of aluminium industry," Open Ceram., **2021**, 7, 1-8. doi: 10.1016/j.oceram.2021.100163.
4. Lawane, A.; Pantet, A.; Vinai, R. and Hugues, J. "Etude géologique et géomécanique des latérites de Dano (Burkina Faso) pour une utilisation dans l'habitat," XXIXe Recontres Univ. Genie Civ., **2011**, 206–215.
5. Bourman R. P. and Ollier, C. D. "A critique of the Schellmann definition and classification of 'laterite,'" Catena, **2002**, 47, 117–131. doi: 10.1016/S0341-8162(01)00178-3.
6. Maiti, A.; Thakur, B. K.; Basu, J. K. and De, S. "Comparison of treated laterite as arsenic adsorbent from different locations and performance of best filter under field conditions," J. Hazard. Mater., **2013**, 262, 1176–1186. doi: 10.1016/j.jhazmat.2012.06.036.
7. Huang, W. Y.; Zhu, R. H.; He, F.; Li, D.; Zhu, Y. and Zhang, Y. M. "Enhanced phosphate removal from aqueous solution by ferric-modified laterites: Equilibrium, kinetics and thermodynamic studies," Chem. Eng. J., 2013, 228, 679–687. doi: 10.1016/j.cej.2013.05.036.
8. Nguyen, T.H.; Tran, H. N.; Vu, H. A.; Trinh, M. V.; Nguyen, T. V.; Loganathan, P. ; Vigneswaran, S.;. Nguyen, T. M; Trinh, V. T.; Vu, D. L. and Nguyen, T. H. H. "Laterite as a low-cost adsorbent in a sustainable decentralized filtration system to remove arsenic from groundwater in Vietnam," Sci. Total Environ., **2020**, 699, 1-11. doi: 10.1016/j.scitotenv.2019.134267.
9. Nguyena, T. H.; Nguyen, A. T.; Loganathan, P.; Nguyen, T. V.; Vigneswaran, S.; Nguyen, T.H. H. and Trand, H. N. "Low-cost laterite-laden household filters for removing arsenic from groundwater in Vietnam and waste management," Process Saf. Environ. Prot., **2021**, 152, 154–163. doi: 10.1016/j.psep.2021.06.002.
10. Thanakunpaisit, N.; Jantarachat, N. and Onthong, U. "Removal of Hydrogen Sulfide from Biogas using Laterite Materials as an Adsorbent," Energy Procedia, **2017**, 138, 1134 –1139. doi: 10.1016/j.egypro.2017.10.215.
11. Kamagate, M.; Assadi, A. A.; Kone, T.; Giraudet, S.; Coulibaly, L. and Hanna, K. "Use of laterite as a sustainable catalyst for removal of fluoroquinolone antibiotics from contaminated water," Chemosphere, **2018**, 195, 847–853. doi: 10.1016/j.chemosphere.2017.12.165.
12. Karki, S.; Timalsina, H.; Budhathoki, S. and Budhathoki, S. "Arsenic removal from groundwater using acid-activated laterite," Groundw. Sustain. Dev., **2022**, 18, 1-13. doi: 10.1016/j.gsd.2022.100769.
13. Millogo, Y.; Traoré, K.; Ouedraogo, R.; Kaboré, K.; Blanchart, P. and Thomassin, J. H. "Geotechnical, mechanical, chemical and mineralogical characterization of a lateritic gravels of Sapouy (Burkina Faso) used in road construction," Constr. Build. Mater., **2008**, 22, 70–76. doi: 10.1016/j.conbuildmat.2006.07.014.
14. Lawane, A.; Vinai, R. ; Pantet, A.; Thomassin, J.-H.; and Messan, A. "Hygrothermal Features of Laterite Dimension Stones for Sub-Saharan Residential Building Construction," J. Mater. Civ. Eng., **2014**, 1–8. doi: 10.1061/(asce)mt.1943-5533.0001067.

15. Maji, S. K.; Pal, A.; Pal, T. and Adak, A. "Adsorption Thermodynamics of Arsenic on Laterite Soil," J. Surf. Sci. Technol., **2007**, 22, 161–176.
16. Maiti, A.; Dasgupta, S.; Basu, J. and De, S. "Adsorption of arsenite using natural laterite as adsorbent," Sep. Purif. Technol., **2007**, 55, 350–359. doi: 10.1016/j.seppur.2007.01.003.
17. Kadam, A. M.; Nemade, P. D.; Oza, G. H. and Shankar, H. S. "Treatment of municipal wastewater using laterite-based constructed soil filter," Ecol. Eng., **2009**, 35, 1051–1061. doi: 10.1016/j.ecoleng.2009.03.008.
18. Xu, D.; Tan, X. L. ; Chen, C. L. and Wang, X. K. "Adsorption of Pb(II) from aqueous solution to MX-80 bentonite: Effect of pH, ionic strength, foreign ions and temperature," Appl. Clay Sci., **2008**, 41, 37–46. doi: 10.1016/j.clay.2007.09.004.
19. Eren E. and Afsin, B. "An investigation of Cu(II) adsorption by raw and acid-activated bentonite: A combined potentiometric, thermodynamic, XRD, IR, DTA study," J. Hazard. Mater., **2008**. 151, 682–691. doi: 10.1016/j.jhazmat.2007.06.040.
20. Melichová Z. and Hromada, L. "Adsorption of Pb2+ and Cu^{2+} Ions from Aqueous Solutions on Natural Bentonite," Polish J. Environ. Stud., **2012**, 22, 457–464.
21. Moutou, J. M.; Foutou, P. M.; Matini, L.; Samba, V. B.; Mpissi, Z. F. D. and Loubaki, R. "Characterization and Evaluation of the Potential Uses of Mouyondzi Clay," J. Miner. Mater. Charact. Eng., **2018**, 06, 119–138. doi: 10.4236/jmmce.2018.61010.
22. Maiti, A.; DasGupta, S.; Basu, J. K. and De, S. "Batch and Column Study: Adsorption of Arsenate Using Untreated Laterite as Adsorbent," Ind. Eng. Chem. Res., **2008**. 47, 1620–1629. doi: 10.1021/ie070908z.
23. Ghani, U.; Hussain, S.; Noor-ul-Amin, Imtiaz, M. and Ali Khan, S. "Laterite clay-based geopolymer as a potential adsorbent for the heavy metals removal from aqueous solutions," J. Saudi Chem. Soc., **2020**, 24, 874–884. doi: 10.1016/j.jscs.2020.09.004.
24. He, F.; Ma, B.; Wang, C.; Chen, Y. and Hu, X. "Adsorption of Pb(II) and Cd(II) hydrates via inexpensive limonitic laterite: Adsorption characteristics and mechanisms," Sep. Purif. Technol., **2023**, 310, 1-13. doi: 10.1016/j.seppur.2023.123234.
25. Mitra, S.; Thakur, L. S.; Rathore, V. K. and Mondal, P. "Removal of Pb(II) and Cr(VI) by laterite soil from synthetic waste water: single and bi-component adsorption approach," Desalin. Water Treat., **2016**. 57, 18406 –18416. doi: 10.1080/19443994.2015.1088806.
26. Mohapatra, M.; Khatun, S. and Anand, S. "Kinetics and thermodynamics of lead (II) adsorption on lateritic nickel ores of Indian origin," Chem. Eng. J., **2009**, 155,184–190. doi: 10.1016/j.cej.2009.07.035.
27. Nayanthika, I. V. K.; Jayawardana, D. T. ; Bandara, N. J. G. J.; Manage, P. M. and Madushanka, R. M. T. D. "Effective use of iron-aluminum rich laterite based soil mixture for treatment of landfill leachate," Waste Manag., 2018, 74, 347–361. doi: 10.1016/j.wasman.2018.01.013.
28. ALzaydien, A. S. "Adsorption of methylene blue from aqueous solution onto a low-cost natural Jordanian Tripoli," Am. J. Appl. Sci., **2009**, 6, 1047–1058. doi: 10.3844/ajassp.2009.1047.1058.
29. Kloprogge, J. T.; Frost, R. L. and Hickey, L. "Infrared emission spectroscopic study of the dehydroxylation of some hectorites," Thermochim. Acta, **2000**, 345, 145–156. doi: 10.1016/S0040-6031(99)00359-7.
30. Ristić, M.; Musić, S. and Godec, M. "Properties of γ-FeOOH, α-FeOOH and α-Fe2O3 particles precipitated by hydrolysis of Fe^{3+} ions in perchlorate containing aqueous solutions," J. Alloys Compd., **2006**, 417, 292–299. doi: 10.1016/j.jallcom.2005.09.043.
31. Lakshmipathiraj, P.; Narasimhan, B. R. V.; Prabhakar, S. and Raju, G. B. "Adsorption of arsenate on synthetic goethite from aqueous solutions," J. Hazard. Mater., **2006**, 136, 281–287. doi: 10.1016/j.jhazmat.2005.12.015.
32. Konan, K. L. "Interactions entre des matériaux argileux et un milieu basique riche en calcium," Thèse de l'Université de Limoge Fr., **2006**, 1–144,
33. Sorgho, B; Paré, S.; Guel, B.; Zerbo, L.; Traoré, K. and Persson I. "Etude d'une argile locale du Burkina Faso à des fins de décontamination en Cu^{2+}, Pb^{2+} et Cr^{3+}," J. la Société Ouest-Africaine Chim., **2011**, 31, 49–59.
34. Maiti, A.; Sharma, H.; Basu, J. K. and De, S. "Modeling of arsenic adsorption kinetics of synthetic and contaminated groundwater on natural laterite," J. Hazard. Mater., **2009**, 172, 928–934. doi: 10.1016/j.jhazmat.2009.07.140.

 doi:10.20944/preprints202502.2150.v1

35. Maiti, A.; Basu, J. K. and De, S. "Experimental and kinetic modeling of As(V) and As(III) adsorption on treated laterite using synthetic and contaminated groundwater: Effects of phosphate, silicate and carbonate ions," Chem. Eng. J., 2012, 191, 1–12. doi: 10.1016/j.cej.2010.01.031.
36. Maji, S. K.; Pal, A. and Pal, T. "Arsenic removal from real-life groundwater by adsorption on laterite soil.," J. Hazard. Mater., **2008**, 151, 811–20. doi: 10.1016/j.jhazmat.2007.06.060.
37. Glocheux, Y.; Pasarín, M. M.; Albadarin, A. B.; Allen, S. J. and Walker, G. M. "Removal of arsenic from groundwater by adsorption onto an acidified laterite by-product," Chem. Eng. J., **2013**,. 228, 565–574. doi: 10.1016/j.cej.2013.05.043.
38. Partey, F.; Norman, D.; Ndur, S. and Nartey, R. "Arsenic sorption onto laterite iron concretions: Temperature effect," J. Colloid Interface Sci., **2008**, 321, 493–500. doi: 10.1016/j.jcis.2008.02.034.
39. Partey, F.. Norman, D. I.; Ndur, S. and Nartey, R. "Mechanism of arsenic sorption onto laterite iron concretions," Colloids Surfaces A Physicochem. Eng. Asp., 2009. 337, 164–172. doi: 10.1016/j.colsurfa.2008.12.018.
40. Rathore, V. K.; Dohare, D. K. and Mondal, P. "Competitive adsorption between arsenic and fluoride from binary mixture on chemically treated laterite," J. Environ. Chem. Eng., **2016**. 4, 2, 2417–2430. doi: 10.1016/j.jece.2016.04.017.
41. Chatterjee, S.; Mondal, S. and De, S. "Design and scaling up of fixed bed adsorption columns for lead removal by treated laterite," J. Clean. Prod., **2018**, 177, 760–774. doi: 10.1016/j.jclepro.2017.12.249.
42. Lawrinenko M. and Laird, D. A. "Anion exchange capacity of biochar," Green Chem., **2015**, 17, 4628–4636, 2015, doi: 10.1039/c5gc00828j.
43. Schell W. R. and Jordan, "Anion-exchange studies of pure clays," Plant Soil, **1959**, 10, 303–318. doi: 10.1007/BF01666207. J. V.
44. Njopwouo, D. and ORLIAC; M. "Note sur le comportement de certains minéraux à l 'attaque triacide," Cah. ORSTOM, sbr. Pedol, **1979**, 17, 329–337.
45. LAIBI, A. B.; GOMINA,M.; SORGHO, B.; SAGBO,E.; BLANCHART,P.; BOUTOUIL, M. and SOHOUNHLOULE, D. K. C. "Caractérisation physico-chimique et géotechnique de deux sites argileux du Bénin en vue de leur valorisation dans l'éco-construction," Int. J. Biol. Chem. Sci., **2017**, 11, 499-514. doi: 10.4314/ijbcs.v11i1.40.
46. Zelazny, L. W. and He, L. "Chapter 41 Charge Analysis of Soils and Anion Exchange," Methods Soil Anal. Part 3. Chem. Methods-SSSA B. Ser. **1996**, 5, 1231–1253.
47. Gallios, G. P.; Tolkou, A. K.; Katsoyiannis, I. A.; Stefusova, K.; Vaclavikova, M. and Deliyanni, E. A."Adsorption of arsenate by nano scaled activated carbon modified by iron and manganese oxides," Sustain., **2017**, 9, 1–18. doi: 10.3390/su9101684.
48. Nemade, P. D.; Kadam, A. M.; Shankar, H. S. and Bengal, W. "Adsorption of arsenic from aqueous solution on naturally available red soil," J. Environ. Biol., **2009**, 30, 499–504.
49. Sanou, Y.; Pare, S.; Nguyen, T.T. and Phuoc, N.V. "Experimental and Kinetic modeling of As (V) adsorption on Granular Ferric Hydroxide and Laterite," J. Environ. Treat. Tech., **2016**, 4, 62–70.
50. Nguyen, P. T. N.; Abella, L. C.; Gaspillo, P. D. and Hinode, H. "Removal of arsenic from simulated groundwater using calcined laterite as the adsorbent," J. Chem. Eng. Japan, **2011**, 44, 411–419. doi: 10.1252/jcej.11we025.
51. Ouedraogo, R.D. ; Bakouan, C. ; Sakira, A.K. ; Sorgho, B. ; Guel, B. ; Somé, T.I. ; Hantson, A.L. ; Ziemons, E. ; Mertens, E. ; Hubert, P. and Kauffmann, J.M. '' The Removal of As(III) Using a Natural Laterite Fixed-Bed Column Intercalated with Activated Carbon: Solving the Clogging Problem to Achieve Better Performance'', *Separations*, **2024**, *11*, 129, 1-27. doi.org/10.3390/separations11040129
52. Uddin, M. K. "A review on the adsorption of heavy metals by clay minerals, with special focus on the past decade," Chem. Eng. J., **2017**, 308, 438–462. doi: 10.1016/j.cej.2016.09.029.
53. Gu, S.; Kang, X.; Wang, L.; Lichtfouse, E. and Wang, C. "Clay mineral adsorbents for heavy metal removal from wastewater: a review," Environ. Chem. Lett., **2019**, 17, 629–654. doi: 10.1007/s10311-018-0813-9.
54. Cheng, C. H.; Lehmann, J. and Engelhard, M. H. "Natural oxidation of black carbon in soils: Changes in molecular form and surface charge along a climosequence," Geochim. Cosmochim. Acta, **2008**, 72, 1598–1610. doi: 10.1016/j.gca.2008.01.010.

55. Achour S. and Youcef, L. "Elimination Du Cadmium Par Adsorption Sur Bentonites Sodique et Calcique," Larhyss J., **2003**, 68–81.
56. Youcef L. and Achour, S. "Elimination du cuivre par des procédés de précipitation chimique et d'adsorption," Courr. du Savoir-**2006**, 59–65.
57. Alshaebi, F. Y., Yaacob, W. Z. W. and Samsudin, A. R. "Removal of arsenic from contaminated water by selected geological natural materials," Aust. J. Basic Appl. Sci., **2010**, 4, 4413–4422.
58. Ghorbel-Abid, I.; Galai, K. and Trabelsi-Ayadi, M. "Retention of chromium (III) and cadmium (II) from aqueous solution by illitic clay as a low-cost adsorbent," Desalination, **2010**, 256, 190–195. doi: 10.1016/j.desal.2009.06.079.
59. Tekin, N.; Kadinci, E.; Demirbaş, Ö.; Alkan, M. and Kara, A. "Adsorption of polyvinylimidazole onto kaolinite," J. Colloid Interface Sci., **2006**, 296, 472–479. doi: 10.1016/j.jcis.2005.09.049.
60. Ayari, F.; Srasra, E. and Trabelsi-Ayadi, M. "Characterization of bentonitic clays and their use as adsorbent," Desalination, **2005,** 185, 391–397. doi: 10.1016/j.desal.2005.04.046.
61. Kouadio, L.M.; Lebouachera, S.I.; Blanc, S.; Sei, J.; Miqueu, C.; Pannier, F. and Martinez, H. "Characterization of Clay Materials from Ivory Coast for Their Use as Adsorbents for Wastewater Treatment," J. Miner. Mater. Charact. Eng., **2022**, 10, 319–337. doi: 10.4236/jmmce.2022.104023.
62. Zhang, X.; Hong, H.; Li, Z.; Guan, J. and Schulz, L. "Removal of azobenzene from water by kaolinite," J. Hazard. Mater., **2009**, 170, 1064–1069. doi: 10.1016/j.jhazmat.2009.05.073.
63. Mbumbia, L.; De Wilmars A. M., and Tirlocq, J. "Performance characteristics of lateritic soil bricks fired at low temperatures: A case study of Cameroon," Constr. Build. Mater., **2000**, 14, 121–131. doi: 10.1016/S0950-0618(00)00024-6.
64. Jahan, N.; Guan, H .and Bestland, E. A. "Arsenic remediation by Australian laterites," Environ. Earth Sci., 2011, 64, 247–253. doi: 10.1007/s12665-010-0844-4.
65. Joussein, E.; Petit, S. and Decarreau, A. "Une nouvelle méthode de dosage des minéraux argileux en mélange par spectroscopie IR," Comptes Rendus l'Academie Sci. - Ser. IIa Sci. la Terre des Planetes, **2001**, 332, 83–89, 2001, doi: 10.1016/S1251-8050(01)01511-7.
66. Madejová, J. "FTIR techniques in clay mineral studies," Vib. Spectrosc., **2003**, 31, 1–10. doi: 10.1016/S0924-2031(02)00065-6.
67. Chen, Y. F.; Wang, M. C.; and Hon, M. H. "Phase transformation and growth of mullite in kaolin ceramics," J. Eur. Ceram. Soc., **2004**, 24, 2389–2397. doi: 10.1016/S0955-2219(03)00631-9.
68. Sarkar, M.; Banerjee, A.; Pramanick, P. P. and Sarkar, A. R. "Design and operation of fixed bed laterite column for the removal of fluoride from water," Chem. Eng. J., **2007**, 1, 329–335. doi: 10.1016/j.cej.2006.12.016.
69. Pham, T. D.; Pham, T. T.; Phan, M. N.; Ngo, T. M. V.; Dang, V. D. and Vu, C. M. "Adsorption characteristics of anionic surfactant onto laterite soil with differently charged surfaces and application for cationic dye removal," J. Mol. Liq., **2020**, 301, 1-9. doi: 10.1016/j.molliq.2020.112456.
70. Rathore, V. K.; Dohare, D. K.; and Mondal, P. "Competitive adsorption between arsenic and fluoride from binary mixture on chemically treated laterite," J. Environ. Chem. Eng., **2016**, 4, 2417–2430. doi: 10.1016/j.jece.2016.04.017.
71. Chatterjee S. and De, S. "Application of novel, low-cost, laterite-based adsorbent for removal of lead from water: Equilibrium, kinetic and thermodynamic studies," J. Environ. Sci. Heal. - Part A Toxic/Hazardous Subst. Environ. Eng., **2016**, 51, 193–203. doi: 10.1080/10934529.2015.1094321.
72. Zhu, D.; He,Y.; Zhang, B.; Zhang, N.; Lei, Z.; Zhang, Z.; Chen, G. and Shimizu, K. "Simultaneous removal of multiple heavy metals from wastewater by novel plateau laterite ceramic in batch and fixed-bed studies," J. Environ. Chem. Eng., **2021**, 9, 1–9. doi: 10.1016/j.jece.2021.105792.
73. Bakouan, C. Caractérisation de Quelques Sites Latéritiques du Burkina Faso: Application à L'élimination de L'arsenic (III) et (V) Dans Les Eaux Souterraines. Thèse de Doctorat en Cotutelle Entre l'Université Ouaga I Pr JKZ et de, l'Université de Mons en Belgique. **2018**, pp. 1–241. Available online: https://orbi.umons.ac.be/bitstream/20.500.12907/31806/1/Th%C3%A8se (accessed on 1 February 2018).

 doi:10.20944/preprints202502.2150.v1